Journal of Materials Chemistry B

Accepted Manuscript

ROYAL SOCIETY OF CHEMISTRY

www.rsc.org/materialsB

Journal of Materials Chemistry B RSCPublishing

ARTICLE

Polypyrrole Stabilized Gold nanorods with Enhanced Photothermal Effect towards Two-Photon Photothermal Therapy

Cite this: DOI: 10.1039/xoxxoooooox

Received,
Accepted

DOI: 10.1039/xoxxoooooox

www.rsc.org/

Cuiling Du[a], Anhe Wang[a], Jinbo Fei[b], Jie Zhao[b] and Junbai Li[a,b]*

The core-shell composite of polypyrrole (PPy) coating on Au nanorods with high two-photon photothermal efficiency and well photostability have been fabricated *via* a facile interfacial polymerization. The relevant transmission electron microscope has confirmed the core-shell structure of the uniform Au-PPy nanorods. The core-shell composites improve the temperature elevation and photostability compared with pure Au nanorods. The composites internalized by cancer cells can be detected by strong two-photon fluorescence thereby minimizing photothermal damage to normal tissues. The cell cytotoxicity and two-photon efficiency experiments *in vitro* demonstrate that the composites of Au-PPy nanorods have high efficiency to inhibit tumor cell proliferation.

1. Introduction

Due to the noninvasive and localized approaches, photothermal therapy has been proved to be a promising treatment in the past few years.[1-5] The near-infrared (NIR) light in the range of 700 to 1000 nm was the optimum condition for photothermal therapy due to the high transparency of tissue.[5,6] Nanomaterials based on the NIR light induced heating conversion have attracted much attention in recent years.[7] Many of the photothermal nanomaterials including inorganic materials, polymers and carbon materials have been widely explored owing to their high optical extinction coefficients in the NIR wavelength range.[5, 8-13] Gold based nanomaterials such as Au nanoshell, nanorods, and nanocages have been proved to be good photothermal agents because the local temperature around gold nanoparticles can be increased by laser illumination in controllable manner through the tunable surface plasmon bands in the NIR region.[14-16] Moreover, gold rods with an excellent biocompatibility and low cytotoxicity showed strong two-photon activity in cellular imaging, which can avoid photoblinking or photobleaching under laser irradiation.[17,18] There are some advantages of the multiphoton microscopy over conventional confocal microscopy, for example, the photobleaching can be reduced by selective excitation of the focal volume, and the depth penetration in scattering samples can be improved by using excitation light within the optical transmission window of biological tissues (NIR spectral range, 700-1000 nm).[19, 20] However, the NIR absorbance peak of Au nanorods would diminish after the irradiation due to the "melting effect".[21] The low photostability or the often-observed clustering and aggregating limited the wide application of Au nanorods. The diversified architectures of self-assembly and co-assembly [22,23] of Au nanorods with mesoporous silica,[24, 25] biomolecule[16] and polymer[26, 27] have been explored to enhance the structural stability and improve the subsequent function. Polypyrrole (PPy) has great application in bioelectronics and biomedical field owing to their high conductivity, good biocompatibility and outstanding stability. [28, 29] Currently, PPy has been reported to be used as optical coherence tomography contrast agent for tumor imaging since their wide range of NIR absorption, which can be extend beyond 1300 nm.[30] Afterwards, it was found that the strong absorption of PPy nanoparticles in the NIR region can create significant photothermal effect. Very recently, PPy nanoparticles have been successfully used as a stable photothermal coupling agent with a high efficiency to kill cancer cells.[5, 8, 31]

In this work, Au nanorods was coated with polypyrrole *via* a facile interfacial polymerization of pyrrole monomer to get high efficient and stable photothermal self-assembly architecture. The overall synthetic procedure is schematically illustrated in Figure 1. After coating, the photostability and the photothermal efficiency are enhanced, meanwhile, lead the characteristic absorption peak a significant red shift to the NIR region. With the detected strong two-photon photoluminescence in tumor cells, the photothermal damage to normal tissue could avoid in some degree. The *in vitro* cell experiment proves that the core-shell composite can efficiently inhibit cancer cell proliferation, which has promising application in the cancer therapy.

[a] *National Center for Nanoscience and Technology, Zhong guan cun, Beijing, 100190 China*
E-mail: jbli@iccas.ac.cn
[b] *Beijing National Laboratory for Molecular Sciences, Key Laboratory of Colloid, Interface Science and Chemical Thermodynamics, Institute of Chemistry, Chinese Academy of Sciences, Beijing 100190 China*

Electronic supplementary information (ESI) available. See DOI: 10.1039/

2. Experimental

2.1. Materials

$AgNO_3$, Pyrrole, Sodium dodecylsulfate (SDS), Ammonium persulfate (APS), $NaBH_4$ and $HAuCl_4.3H_2O$ were obtained from Beijing Chemical Reagent Ltd., China. Ascorbic acid, Nile red, Hexadecyltrimethylammonium bromide (CTAB) and Hoechst 33342 were obtained from Sigma-Aldrich. 3-(4,5-Dimethylthiazolyl-2)-2,5-diphenyl tetrazolium bromide (MTT) was purchased from Amresco. Alexa Fluor 488 was obtained from Molecular Probes Inc. All the materials were commercially available and used as received without further purification. The water used in all experiments was prepared in a Milli-QPlus 185 purification system (Millipore) with aresistivity of 18.2 MΩ·cm.

2.2. Synthesis of Au nanorods

A colloidal Au nanorods sample was prepared using a seed-mediated method in CTAB aqueous solutions. The seed solution was made as following, $NaBH_4$ solution (0.12 mL, 0.01M) was added to the mixture solution of $HAuCl_4$ (0.05 ml, 0.01M) and CTAB (1.5 mL, 0.1M). Then, the mixed solution was kept at room temperature for at least 2 h before use. The growth of Au nanorods was carried out firstly by mixing CTAB (80 mL, 0.1M), $HAuCl_4$ (4 mL, 0.01M), $AgNO_3$ (1 mL, 0.01M), freshly prepared ascorbic acid solution (0.8mL, 0.1M), HCl (1mL, 1M) together. Secondly, the seed solution (0.2 mL) was added. Then, the mixed solution was left in a water bath for 10 h keeping the temperature around 28 ^oC.

2.3. Synthesis of Au-PPy composites

The coating on the Au nanorods was proceeding as below. Firstly, the prepared Au nanorods solution (4 mL) was centrifuged and washed for twice. The precipitate was redispersed in 2 mL water solution. Secondly, the mixture of pyrrole monomer (1 μM or 10 μM) and SDS (10 μM) were added in the dispersion stirring for 30 min. After the addition of APS (0.8 μM or 8 μM), the reaction mixture was stirring for 24 h to ensure the polymerization complete. Then the mixture was centrifugated and washed for use. The repeat coating experiment was carried out with the same method for the second time.

2.4. Characterization

The morphologies of the samples were examined by TEM conducted with a JEOL 2011 transmission electronic microscope working at 200 kV. The elemental components were analyzed by an EDX analyzer as the SEM accessory. A Hitachi U-3010 spectrophotometer was used to record the UV-vis spectra. One-photon and two-photon fluorescence images were obtained by a two-photon laser scanning microscope (CLSM, Olympus FV500, Olympus FV500 with 60× and 100× oil-immersion objectives and a numerical aperture of 1.35).

2.5. Cell Culture and Cytotoxicity Assay

The human cervical cancer cell line (HeLa) was used for intracellular localization. The cells were cultured in DMEM medium at 37 °C in 5% CO_2 with 70% humidity. 10% fetal calf serum, 1% penicillin and streptomycin were contained in DMEM medium. When the cells reached about 90% confluency, they were split into a 35 mm Petri dish using a standard trypsin-based technique for imaging. When the cells were cultured in DMEM medium for 24 h, 20 μL Au-PPy suspension was added to Petri dish for co-culturing for 24 h. After the removing of the Au-PPy nanorods and dead cells, Alexa Fluor 488 and Hoechst 33342 (10 μL, 50 mg mL^{-1}) were employed for stain the membrane and cell nucleus, respectively. Then the cells could be observed by CLSM.

The human cervical cancer cell line (HeLa) was used for cytotoxicity studies. HeLa cells were split into 48-well plates using a standard trypsin-based technique with a final concentration of 5 × 10 4 cells mL^{-1}. When cells in 48-well plates were cultured at a concentration about 90% confluence, Au-PPys (at Au-equivalent does) with different concentration (0, 5.8, 11.6, 23.2 and 46.4 μg mL^{-1}) were added to per well and incubated for 24 h. The culture medium was changed to remove the Au-PPy that was not taken up by cells. The cells were irradiated with 808 nm light for 3 min and further incubated for 12 h. Cell survival was investigated by the standard MTT assay. In detail, cellular culture medium was removed and replaced. MTT (20 μL; 5 mg mL^{-1}) in PBS was added to each well and incubated with the cells at 37 °C for 4 h. The remaining MTT was removed and dimethyl sulfoxide (DMSO, 200 μL in every well) was added to dissolve the purple formazan crystals, and then measured at a wavelength of 490 nm absorbance by a wallac 1420 multilabel counter.

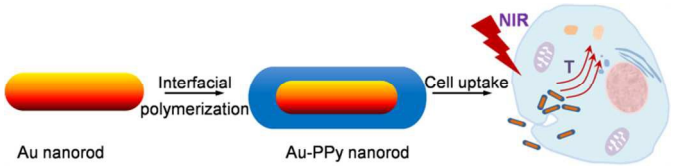

Figure 1. The fabrication of Au-PPy composite nanorods and their application in cancer imaging and therapy by one-photon or two-photon laser.

3. Results and discussion

3.1. Preparation and Characterization of Au-PPy nanorods

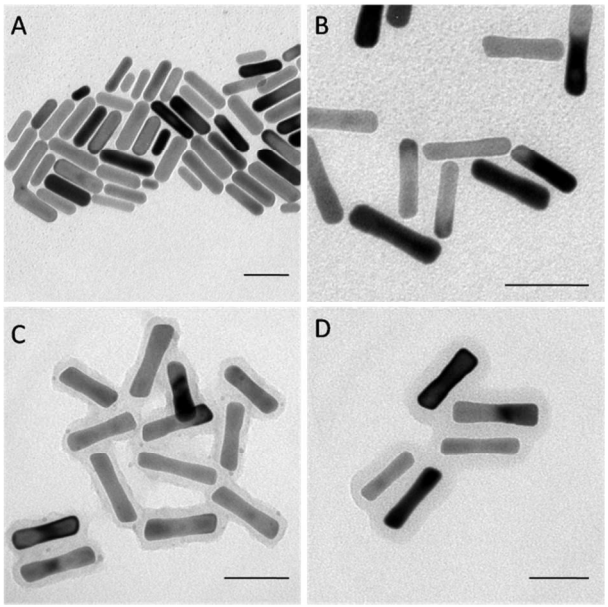

Figure 2. TEM images of Au nanorods (A), and Au-PPy nanorods fabricated with the doses of pyrrole monomer 1 μM (B); 10 μM (C); 10 μM repeat twice (D). All scale bars are 50 nm.

Au nanorods were prepared by using a seed-mediated method as

described in the Experiment Method. Figure 2 have shown the TEM images of the as-prepared Au nanorods and Au-PPy nannorods with different conditions. As shown in the Figure 2A, the average diameter and length of the Au nanorods were about 15 nm and 50 nm. After pyrrole monomer polymerized on the surface of the Au nanorods, the morphology differences can be seen in Figure 2B, 2C and 2D, respectively. The coating shells thicknesses could be increased with the increasing of concentration or coating times from very thin to about 8 nm or 13 nm. The coating of PPy was realized through surfactant-assisted chemical oxidative polymerization.[27, 32] In this process, sodium dodecylsulfate (SDS), an anionic surfactant can be adsorbed on the CTAB layers on the surface of the Au nanorods through electrostatic interaction. Then pyrrole monomers were trapped within the surfactant layers. Ultimately, with the addition of the oxidant, ammonium persulfate (APS), the polymerization of pyrrole were occurred. During the polymerization process, the introduced surfactant SDS stabilizes the Au nanorods to prevent the aggregation. [27]

After coating, the color changes of the solution and the surface plasmon resonance feature have been shown in Figure 3A and 3B. Figure 3A was the photo images of the Au nanorods (a) and the Au-PPy nanorods (b, c and d) solution corresponding to Figure 2 with equal Au concentration of 0.2 mg/mL, respectively. The color of the solution before coating was wine red, while the color becomes darker and darker after the polymerization of PPy with the coating thickness increasing. In addition, the zeta-potential of the Au-PPy nanorods in water solution (about pH 7) decreased from 12.3±1.5 to -13.9±0.4 mV. The negative charges on their surface might be due to the doping of SDS.[33] The UV-vis spectroscopic studies were preformed to monitor the surface plasmon resonance feature of the Au nanorods and the Au-PPy nanorods solution. The spectrum of Au nanorods had shown the characteristic absorption band at 841 nm (Curve c). However, after coating by the PPy, the surface plasmon peaks shifted to around 876 and 887 nm (Curve a and b) corresponding to Figure 2C and 2D, respectively. The coating of polymer shell makes the electron vibration in the Au nanorods confine in a smaller space, which shortens the extent of electron vibration. Moreover, as a conductive polymer, when PPy is polarized by exposed to external irradiation, the PPy shell can provide additional electrons oscillating with those accounted for the Au surface plasmon resonance. Thus the enhanced restore force and shortened the extent of electron vibration were the reason that the composite structures promoted the red shift of the characteristic absorption peak to NIR. [34, 35]

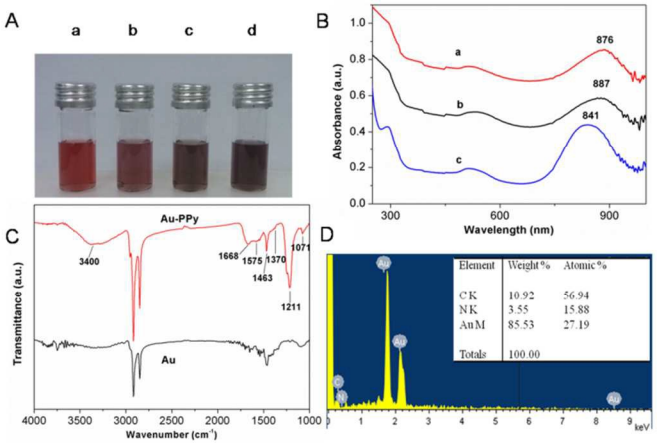

Figure 3. (A) The photo images of Au nanorods (a) and Au-PPy nanorods (b, c, d) water solution. (B) The UV-vis spectra of the Au nanorods (c) and Au-PPy nanorods (a and b). (C) FT-IR spectra of Au nanorods and Au-PPy nanorods; and (D) EDX analysis of Au-PPy nanorods.

To investigate the chemical components, the Au-PPy nanorods and Au nanorods were characterized by Fourier transform infrared (FTIR) and energy dispersive X-ray (EDX) analyzer. As Figure 3C shown, the broad peak centered at 3400 cm^{-1} result from the stretching vibrations of N-H. The peak at 1575 cm^{-1} was assigned to the stretching vibrations of C-C in the pyrrole ring. [36] The bands at 1071 and 1370 cm^{-1} corresponded to the C-H deformation vibrations and C-N stretching vibrations.[37] The band at 1463 cm^{-1} was due to the fundamental stretching vibration of pyrrole rings.[38] The peak at 1211 cm-1 was related to the in-plane vibrations of C-H.[36] Additionally, in order to confirm the PPy was coating on the surface of Au nanorods, the elemental analysis was carried out. The Figure 3D has shown the present elemental components of C, N and Au in the Au-PPy nanorods. In this case, the atomic ratio of N/C was about 1/4. It could be observed that the ratio of 1/4 fits well with the structure of PPy. The results demonstrated that PPy had been coating on the surface of Au nanorods successfully.

3.2. Photothermal Effect and Photostability of Au-PPy nanorods

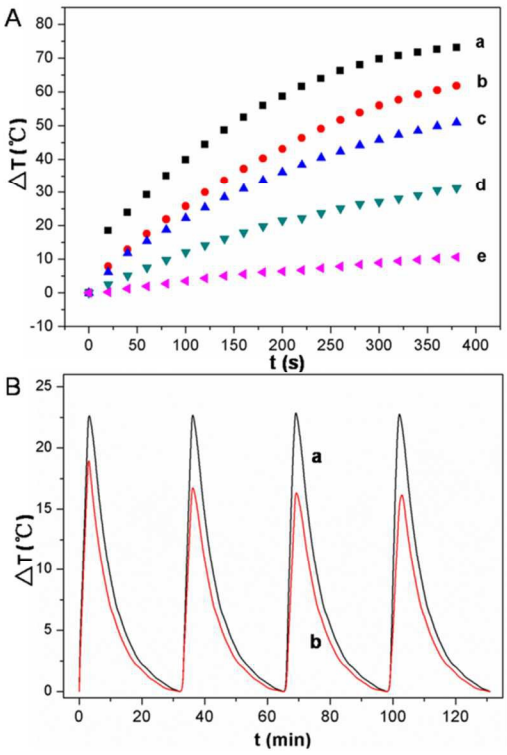

Figure 4. (A) The temperature elevation over a period of 380 s of exposure to a NIR laser (808 nm, 3 W) at different concentations of Au-PPy nanorods (a) 92.8 μg mL^{-1}; (b) 46.4 μg mL^{-1}; (c) 23.2 μg mL^{-1}; (d) 11.6 μg mL^{-1}; (e) 0 μg mL^{-1}; (B) Temperature elevation record of 20 μg mL^{-1} Au-PPy (a) and Au (b) nanorods over four laser on/off cycles by a 3 W, 808 nm laser.

The photothermal effect of Au-PPy nanorods was carried out by monitoring the temperature of 1 mL solution containing various concentrations (equal Au concentration 92.8, 46.4, 23.2, and 11.6 μg mL^{-1}) using a NIR laser (808 nm, 3 W). As shown in Figure 4A, after the irradiation, the solution exhibited a temperature increment with the concentration increase. The Au-PPy solution with different concentration 92.8, 46.4, 23.2 and 11.6 μg mL^{-1} elevate the temperature 73.1, 61.8, 50.8 and 31.2 ^{o}C, respectively. The result indicated that the Au-PPy nanorods possess better photothermal performance. The stability of the solution before and after the irradiation had been monitored by UV-vis spectra (Figure S1A). After heating by NIR laser (808 nm 3 W) irradiation for an hour, there was no significant difference in the adsorption spectrum. The location and the intensity of the maximum peak almost had kept the same after the irradiation. The TEM image in Figure S1B also indicated that the rods structure of Au-PPy had retained well after irradiation. These data had proved that the Au-PPy nanorods stable enough to be used as an efficient photothermal agent.

To compare the Au-PPy nanorods with Au nanorods for their photostability and the photothermal effect, four cycles of irradiation on/off with an 808 nm laser were carried out. With the same equal Au mass concentration (20 μg mL^{-1}), the solutions of Au-PPy naorods and Au nanorods were irradiated for 3 min (ON), then cooling to room temperature without irradiation (OFF). As shown in Figure 4B, the temperature elevation were present as 23.25, 23.33, 23.33 and 23.21 ^{o}C for four repeat times corresponding to Au-PPy naorods (Curve a), in the same condition, whereas the temperature elevation of Au nanorods (Curve b) have changed to 19.71, 17.20, 16.73 and 16.67 ^{o}C, respectively. It was clearly indicated that the composite structure of Au-PPy nanorods showed higher photothermal conversion efficiency than pure Au naorods.[5, 33] The temperature elevation of Au nanorods changed from 19.71 ^{o}C to 16.67 ^{o}C during the four cycles; however, there was no significant decrease was observed for Au-PPy nanorods. The four cycle experiment also proved the photostability of Au-PPy nanorods. The results further confirmed that the Au-PPy nanorods could act as an efficient photothermal agent.

3.3. Photothermal Effect Induced by Au-PPy nanorods *In Vitro*

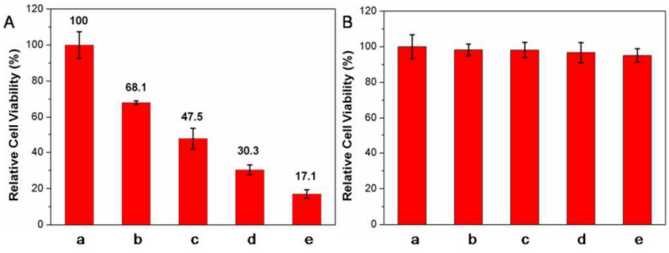

Figure 5. (A) *In vitro* cytotoxicity results with different concentrations (a) negative control experiment; (b) 5.8 μg mL^{-1}; (c) 11.6 μg mL^{-1}; (d) 23.2 μg mL^{-1}; (e) 46.4 μg mL^{-1} with irradiation by a laser (808 nm 3 W) for 3 min. (B) Cell viability data obtained from HeLa cells incubated with Au-PPy at different concentrations for 24 h. (a) negative control experiment; (b) 5.8 μg mL^{-1}; (c) 11.6 μg mL^{-1}; (d) 23.2 μg mL^{-1}; (e) 46.4 μg mL^{-1}.

To further confirm the photothermal effect in cancer therapy, Au-PPy nanorods were incubated with HeLa cells for 24 h at different Au-equivalent dose. After the removal of free Au-PPy nanorods, the cells were irradiated with 808 nm laser for 3 min and further cultured for 12 h. As shown in Figure 5A, it was found that the cell viability was reduced significantly with the increase of concentration, from 68.1 % to 17.1 %. The result indicated that the cytotoxicity of Au-PPy nanorods were concentration dependent under the certain condition of laser intensity. The ideal photothermal agent used in biological system should be nontoxic or lowtoxic. To evaluate the biocompatibility of Au-PPy nanorods without light, the MTT assay was performed. Figure 5B showed that the cells incubated with Au-PPy nanorods at different concentrations had high cell viability. It was demonstrated that Au-PPy nanorods with good biocompatibility could be used as an efficient photothermal agent against tumor cell proliferation.

3.4. Intracellular Distribution of Au-PPy nanorods

To investigate the internalization of Au-PPy nanorods by cancer cells and further evaluate the potential use for *in vitro* imaging with two-photon excitation, Au-PPy nanorods were incubated with HeLa cells. Nile red was used to monitor the internalization of Au-PPy nanorods in the HeLa cells with one-photon excitation. The red fluorescence in Figure 6C was the contribution of Nile red capsulated in the polymer layer excited by 559 nm laser. The red fluorescence in Figure 6D was corresponding to the Au nanorods excited by the two-photon fluorescence microscopy at 880 nm. After incubation, the red fluorescence present in Figure 6C confirmed the taken up of Au-PPy

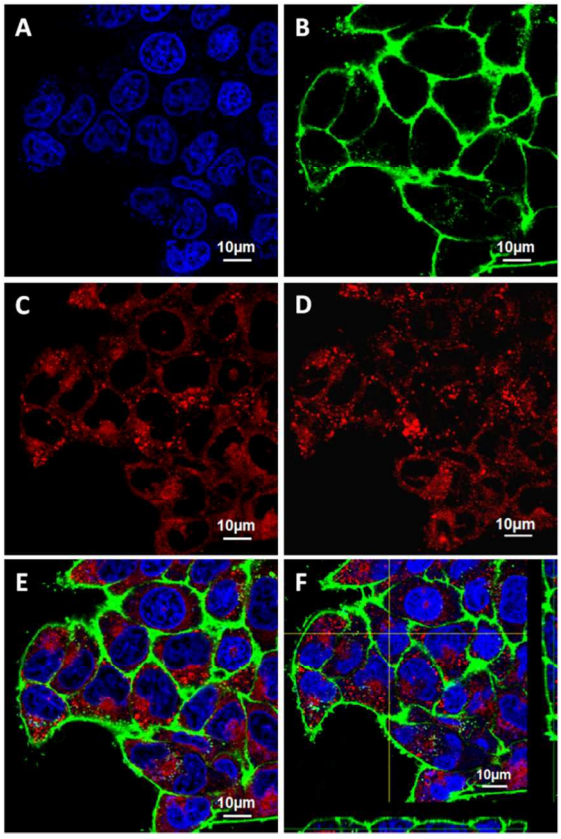

Figure 6. CLSM observation of HeLa cells incubated with Au-PPy nanorods for 24 h. (A) Blue nuclei excited by 405 nm laser stained by Hoechst 33342; (B) Green fluorescence corresponding to the membrane excited by 488 nm laser stained by Alexa 488; (C) Red fluorescence corresponding to Nile red capsulated in the polymer layer of the Au-PPy nanorods internalized by HeLa cells excited by 559 nm. (D) Two-photon luminescence image of Au-PPy naorods scattered in the cytoplasm; (E) The merged image of A, B and C; (F) A 3D CLSM image of HeLa cells was cut to form xz and yz sections. The two yellow lines correspond to xz (bottorm) and yz (right) side views at a given z.

nanorods by HeLa cells. From the overlay image (Figure 6E), it could be observed that the nanorods were distributed in the cytoplasm around the cell nucleus. To further prove the uptake of nanorods, Z-sectioning was performed for identification of nanorods intracellular location. As shown in Figure 6F, the nanorods (red fluorescence) encapsulated by cytomembrane (green fluorescence) could be observed in xz and yz sides by 3D reconstruction to show the cell endocytosis. Additionally, it was notable that there was no detectable fluorescence from Nile red outside the nanorods location, suggesting the premature leaking of the payload did not occur. It was also indicated that the Au-PPy nanorods could be used as drug carriers which had promising application for the combined therapy. Moreover, at this stage, the two-photon image was shown in Figure 6D. The red fluorescence could be attributed to the two-photon photoluminescence of Au nanorods under the plasmon-resonant condition collected in the red channel. Compared with Figure 6C, the location of red fluorescence in Figure 6D did not have significantly differences. It indicated that the composites could be localized in tumor tissues and further internalized by tumor cells,[39] then well detected by two-photon photoluminescence. Meanwhile, the tumor location could be selectively destroyed by a NIR laser thereby minimizing damage to the surrounding normal tissues. The results suggest that the Au-PPy nanorods with the strong two-photon fluorescence and excellent stability might offer great potential for imaging and related biomedical applications, as deep imaging within tissue with high resolution has become possible by two-photon fluorescence microscopy.

Figure 7. The CLSM images of HeLa cells during the time scanning process with a two-photon laser at 880 nm.

3.5. Two-photon Photothermal Effect of Au-PPy nanorods *In Vitro*

To further evaluate the potential use of Au-PPy nanorods as photothermal agent excited by two-photon, Au-PPy nanorods were incubated with HeLa cells for 24 h. After the removal of the nanorods in the cell culture medium, the cells were excited by a two-photon fluorescence microscopy at 880 nm (0.86 J cm^{-2}) with a time scanning. As shown in Figure 7, the image was recorded every 30 s, one can see that the bubble induced by thermal effect came into being, grew bigger and more gradually with time increasing. This indicated that the enhanced local heating effect was time dependent with the certain laser intensity. When time came to 570 s, the cancer cells were destroyed completely. The control experiment without Au-PPy was also carried out at the same condition (Figure S2). The cells morphology almost had no difference during the irradiation of two-photon laser. It was demonstrated that the result of photothermal treatment was caused by the Au-PPy under the two-photon laser rather than the laser damage. The time scanning images clearly demonstrated the cell morphological changes during the process of the photothermal treatment with a two-photon laser and the result vividly proved that photothermal treatment regime by two-photon therapy can dramatically destroy tumor cells *in vitro*.

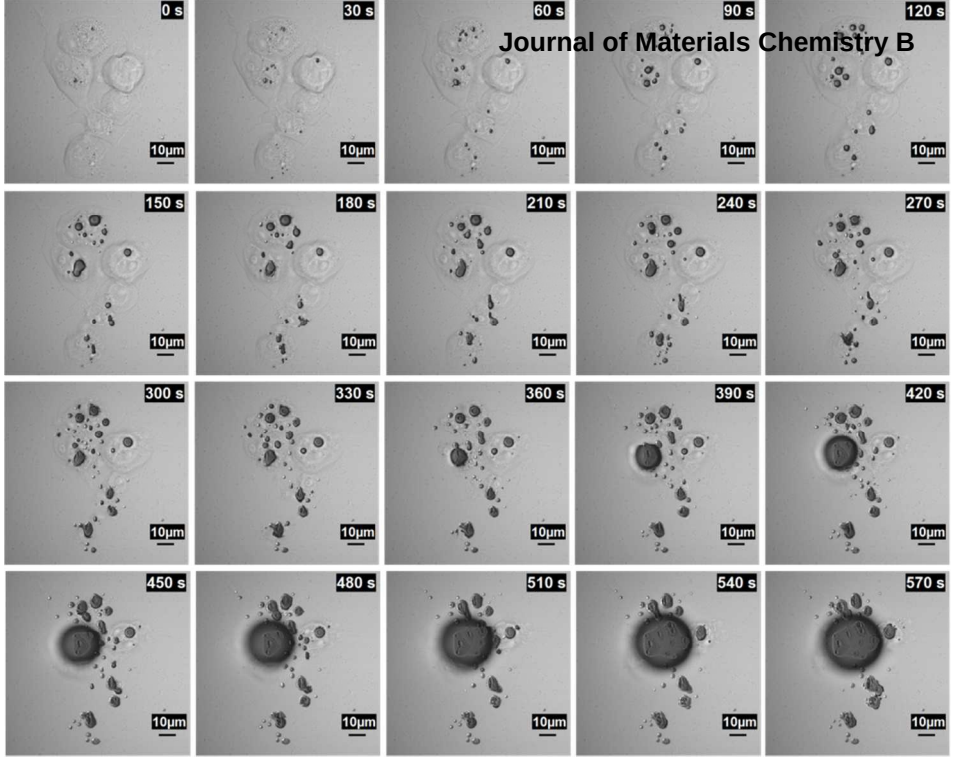

4. Conclusions

In summary, we have successfully developed the Au-PPy core-shell nanorods for two-photon photothermal cancer therapy *in vitro*. The as-prepared complex exhibited good biocompatibility, photostability and enhanced photothermal effect. After the internalization, the composite in cancer cells could be well detected by two-photon microscope which can be used to minimize photothermal damage to normal tissues. The complex nanorods showed high photothermal efficiency to kill cancer cells, which also can be used for drug carrier for combined cancer therapy. Therefore, this core-shell structure with a polymer layer surface and Au nanorods core might create a new type system for cancer therapy, deep imaging, drug delivery, and diagnosis application.

Acknowledgements

This work was financially supported by the National Basic research Program of China (973 Program 2013CB932802), the National Nature Science Foundation of China (21321063, 21303219, 51303038 and 21273250).

Notes and references

[1]A. Vogel and V. Venugopalan, *Chem. Rev.*, 2003, **103**, 2079-2079.
[2] A. M. Gobin, M. H. Lee, N. J. Halas, W. D. James, R. A. Drezek and J. L. West, *Nano. Lett.*, 2007 , **7** , 1929-1934.
[3] C. M. Hessel, V. P. Pattani, M. Rasch, M. G. Panthani, B. Koo, J. W. Tunnell and B. A. Korgel, *Nano. Lett.*, 2011, **11,** 2560-2566.
[4] X. H. Huang, I. H. El-Sayed, W. Qian and M. A. El-Sayed, *J. Am. Chem. Soc.*, 2006, **128**, 2115-2120.
[5] Z. B. Zha, X. L. Yue, Q. S. Ren and Z. F. Dai, *Adv. Mater.*, 2013, **25**, 777-782.
[6] R. Weissleder, *Nat. Biotechnol.*, 2001, **19**, 316-317.
[7] T. L. Doane and C. Burda, *Chem. Soc. Rev.*, 2012, **41**, 2885-2911.
[8] K. Yang, H. Xu, L. Cheng, C. Sun, J. Wang and Z. Liu, *Adv. Mater.*, 2012, **24**, 5586-5592.
[9] M. Chen, X. Fang, S. Tang and N. Zheng, *Chem. Commun.*, 2012, **48**, 8934-8936.
[10] J. W. Kim, E. I. Galanzha, E. V. Shashkov, H. M. Moon and V. P. Zharov, *Nat. Nanotechnol.*, 2009, **4**, 688-694.
[11] M. Li, X. Yang, J. Ren, K. Qu and X. Qu, *Adv. Mater.*, 2012, **24**, 1722-1728.
[12] A. Lee, G. F. S. Andrade, A. Ahmed, M. L. Souza, N. Coombs, E. Tumarkin, K. Liu, R. Gordon, A. G. Brolo and E. Kumacheva, *J. Am. Chem. Soc.*, 2011, **133**, 7563-7570.
[13] Z. Chen, Q. Wang, H. Wang, L. Zhang, G. Song, L. Song, J. Hu, H. Wang, J. Liu, M. Zhu and D. Zhao, *Adv. Mater.*, 2013, **25**, 2095-2100.
[14] L. Gao, J. Fei, J. Zhao, H. Li, Y. Cui and J. Li, *ACS Nano*, 2012, **6**, 8030-8040.
[15] A. Topete, M. Alatorre-Meda, P. Iglesias, E. M. Villar-Alvarez, S. Barbosa, J. A. Costoya, P. Taboada and V. Mosquera, *ACS Nano*, 2014, **8**, 2725-2738.
[16] T. Murakami, H. Nakatsuji, N. Morone, J. E. Heuser, F. Ishidate, M. Hashida and H. Imahori, *ACS Nano*, 2014, **8**, 7370-7376.
[17] C. J. Murphy, A. M. Gole, J. W. Stone, P. N. Sisco, A. M. Alkilany, E. C. Goldsmith and S. C. Baxter, *Acc. Chem. Res.*, 2008, **41**, 1721-1730.
[18] N. Gao, Y. Chen, L. Li , Z. Guan, T. Zhao, N. Zhou, P. Yuan, S. Q. Yao and Q. H. Xu, *J. Phys. Chem. C*, 2014, **118**, 13904-13911.
[19] E. M. Sevick-Muraca, J. P. Houston and M. Gurfinkel, *Curr. Opin. Chem. Biol.*, 2002, **6**, 642-650.
[20] I. Schick, S. Lorenz, D. Gehrig, A. M. Schilmann, H. Bauer, M. Panthofer, K. Fischer, D. Strand, F. Laquai and W. Tremel, *J. Am. Chem. Soc.*, 2014, **136**, 2473-2483.
[21] B. Nikoobakht and M. A. El-Sayed, *Chem. Mater.*, 2003, **15**, 1957-1962.
[22]K. Ariga, Y. Yamauchi, G. Rydzek, Q. Ji, Y. Yonamine, K. Wu and J. P. Hill, *Chem. Lett.* 2014, **43**, 36–68
[23]L. Yao, J. He, *Prog. Mater. Sci.* 2014, **61**, 94-143.
[24] Z. Zhang, L. Wang, J. Wang, X. Jiang, X. Li, Z. Hu, Y. Ji, X. Wu and C. Chen, *Adv. Mater.*, 2012, **24**, 1418-1423.
[25]X. Yang , X. Liu , Z. Liu , F. Pu , J. Ren and X. Qu, *Adv. Mater.* 2012, **24**, 2890–2895.
[26] Z. Shi, W. Ren, A. Gong, X. Zhao, Y. Zou, E. M. B. Brown, X. Chen and A. Wu, *Biomaterials*, 2014, **35**, 7058-7067.
[27] N. Jiang, L. Shao and J. Wang, *Adv. Mater.*, 2014, **26**, 3282-3289.
[28] J. Jang and H. Yoon, *Small*, 2005, **1**, 1195-1199.
[29] W. K. Oh, H. Yoon and J. Jang, *Biomaterials*, 2010, **31**, 1342-1348.
[30] Z. Zha, Z. Deng, Y. Li, C. Li, J. Wang, S. Wang, E. Qu and Z. Dai, *Nanoscale*, 2013, **5**, 4462-4467.
[31] Q. Tian, Q. Wang, K. Yao, B. Teng, J. Zhang, S. Yang and Y. Han, *Small*, 2014, **10**, 1063-1068.
[32] S. X. Xing, L. H. Tan, M. X. Yang, M. Pan, Y. B. Lv, Q. H. Tang, Y. H. Yang and H. Y. Chen, *J. Mater. Chem.*, 2009, **19**, 3286-3291.
[33]J. Li, J. Han, T. Xu, C. Guo, X. Bu, H. Zhang, L. Wang, H. Sun, and B. Yang, *Langmuir,* 2013, 29, 7102−7110
[34] E. Prodan, C. Radloff, N. J. Halas and P. A. Nordlander, *Science*, 2003, **302**, 419-422.
[35] M. Lin, C. Guo, J. Li, D. Zhou, K. Liu, X. Zhang, T. Xu, H. Zhang, L. Wang and B. Yang, *ACS Appl. Mater. Interfaces*, 2014, **6**, 5860-5868.

[36] T. Yao, T. Cui, H. Wang, L. Xu, F. Cui and J. Wu, *Nanoscale*, 2014, **6**, 7666-7674.
[37] X. Zhang, J. Zhang, W. Song and Z. J.Liu, *Phys. Chem. B* 2006, **110**,1158-1165.
[38]W. Zhong, S. Liu, X. Chen, Y. Wang and W. Yang, *Macromolecules* 2006, **39**, 3224-3230
[39] V. P. Chauhan and R. K. Jain, *Nat. Mater.*, 2013, **12**, 958-962.

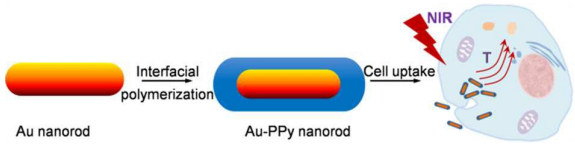

The core-shell composite of Au-polypyrrole nanorods with high two-photon photothermal effect and stability could efficiently kill tumor cells under irradiation.